GOSPODARKA SUROWCAMI MINERALNYMI – MINERAL RESOURCES MANAGEMENT

2024 Volume 40 Issue 4 Pages 47–69

DOI: 10.24425/gsm.2024.152718

JIAJIA MU[1], YUANYUAN LIU[2], YU GUO[3], QIN ZHOU[4]

Recovery of lithium from waste liquid of rock salt brine using aluminum hydroxide precipitation method

Introduction

As the future "white petroleum", lithium is widely applied in chemical power sources, light alloys, metallurgy, medicine, ceramics, lubricants, nuclear materials, and other industries (Li et al. 2019; Meng et al. 2019). In recent years, the demand for lithium has dramatically increased due to the fast development of the new energy vehicle industry, portable electronic products, and energy storage industry (Xu et al. 2020). In 2023, the global demand for lithium has increased to 165 kt, with forecasts as high as 531 kt by 2030 (IEA 2024).

Lithium resources mainly occur in lithium ores (spodumene, lepidolite, and petalite) and salt lake brine. The exploitation and utilization of lithium ore resources have a history of over a hundred years, but the insufficient resource reserves and massive cost of ecological restoration limited its utilization (Liu et al. 2022). The salt lake brine occupied more than

✉ Corresponding Author: Yuanyuan Liu; e-mail: 1076364887@qq.com
[1] 107 Geological and Mineral Exploration Institute, China; ORCID iD: 0009-0000-3063-052X
[2] Yangtze Normal University, China; ORCID iD: 0000-0001-9947-5492; e-mail: 1076364887@qq.com
[3] 107 Geological and Mineral Exploration Institute, China; ORCID iD: 0009-0005-7864-6578
[4] Yangtze Normal University, China; ORCID iD: 0009-0006-9596-2799

70% of lithium reserves. However, the lithium production capacity in salt lake brine has yet to be effectively released due to the resource's various geographical and climatic conditions, which restrict the lithium extraction technology. In China, lithium resources in salt lake brines are mainly distributed in the Qinghai-Tibet Plateau. The high Mg^{2+}/Li^{+}ratio is the main factor restricting the exploitation of lithium resources in Qinghai's salt lakes. In contrast, most of Tibet's lithium salt lakes are located in remote areas with poor infrastructure, harsh alpine, and high altitudes, leading to limited technological research and development industrialization despite the superior resource endowment (Ma and Zhang 1999).

Developing new lithium resources is essential for the increasing demand for lithium and environmental protection. The newly developing lithium resource in this study is the waste liquid from the salt manufacturing plant of the Well Rock salt mine. The lithium concentration of this waste liquid has been enriched to the cut-off grade from only several ppm by cyclic utilization of brine in the salt production process. The annual discharge volumes of waste liquid from rock salt in China were estimated to be more than 500 million tons, reserving about 30,000 tons of lithium carbonate equivalent (the average lithium concentration takes 0.1 g/L for estimation) (NBSC 2023), which can be regarded as a potential lithium resource. Moreover, the convenient transportation, mature infrastructure, and rich human resources relying on the salt manufacturing plant favored the development of lithium recycling from rock salt brine waste liquid, showing an environment-friendly and resource-saving prospect.

The waste liquid from rock salt brine mainly consisted of Na^{+}, K^{+}, Cl^{-}, Ca^{2+}, Mg^{2+}, B^{3+}, and SO_4^{2-} as similar to salt lake brine, but the concentration of these ions existed some differences that Na+ and Cl^{-} concentrations were always close to saturated NaCl solution and some impurities (Ca^{2+}, Mg^{2+}, B^{3+} and SO_4^{2-}) contents were relatively low because the waste liquid needed to be purified before discharge. Due to the similar chemical compositions, the recovery of lithium from the waste liquid of rock salt brine can refer to salt lake brine methods that contain precipitation (Wang et al. 2017; Han et al 2018), adsorption (Li et al. 2020), solar pond (Yu et al. 2014), solvent extraction (Song et al. 2020), membrane (Chung et al. 2008) and electrodialysis methods (Xiong et al. 2021). The precipitation method is a traditional method that uses carbonate (An et al. 2012), aluminate (Zhong et al. 2021), and phosphate (He et al. 2017) to precipitate lithium. In this study, the amorphous $Al(OH)_3$ produced by $AlCl_3 \cdot 6H_2O$ and NaOH was used to precipitate Li^{+} in the waste liquid from rock salt brine with the formation of $LiCl \cdot 2Al(OH)_3 \cdot xH_2O$ salt (Kotsupalo et al. 2013; Paranthaman et al. 2017). The chemical reaction formula of Li^{+} precipitation was as follows.

$$LiCl + 2AlCl_3 + 6NaOH \rightarrow LiCl \cdot 2Al(OH)_3 \cdot xH_2O + 6NaCl \quad (1)$$

Then the $LiCl \cdot 2Al(OH)_3 \cdot xH_2O$ salt was roasted at 400°C to transfer from insoluble to soluble lithium.

$$LiCl \cdot 2Al(OH)_3 \cdot xH_2O \rightarrow LiCl + Al_2O_3 + (x + 3)H_2O \quad (2)$$

The roasted products were then leached by water to obtain the enriched Li^+ solution (~2 g/L), followed by the evaporation treatment to concentrate Li^+ to ≥10 g/L. Finally, the Li_2CO_3 product was precipitated by Na_2CO_3 solution after impurities removal.

$$2Li^+ + Na_2CO_3 \rightarrow Li_2CO_3 + 2Na^+ \quad (3)$$

In the experiments, the influences of Al^{3+}/Li^+ mole ratio, Na^+/Al^{3+} mole ratio, precipitation temperature, and time on the recovery of Li^+ were investigated. Furthermore, thermodynamic analyses of the simulated Li^+–Al^+–Mg^{2+}–Cl^-–H_2O system at 298.15, 313.15, 333.15, and 353.15 K during Li^+ precipitation by $Al(OH)_3$ stage were also conducted to construct the φ-pH diagrams. Subsequently, the roasting process of Li^+ precipitates was carried out to transfer $LiCl \cdot 2Al(OH)_3 \cdot xH_2O$ salt to soluble LiCl, followed by water leaching to obtain the enriched Li^+ solution. Finally, an evaporation process was performed to enhance Li^+ concentration, and the evaporated solution was used to precipitate Li_2CO_3 product by adding Na_2CO_3 after SO_4^{2-}, Ca^{2+} and Mg^{2+} removal.

1. Materials and methods

1.1. Materials and apparatus

The waste liquid was collected from rock salt brine in the salt plant located in Wanzhou District (Chongqing, China). The waste liquid was analysed by ICP-OES (Agilent 5110, USA) to detect its chemical compositions and SO_4^{2-} content was measured by ion chromatography (Dionex ICS-1100, USA). Temperature-controlled water baths with magnetic stirrer (DF-101S, Yuhua instrument) were used in experiments where heating and stirring were required. All chemicals used in this study were of analytical grade.

1.2. Experimental techniques

The recovery of lithium from the waste liquid of rock salt brine adopted the aluminum hydroxide precipitation method, which consisted of Li^+ precipitation by $Al(OH)_3$, roasting, water leaching, evaporation, and Li_2CO_3 precipitation. The flowsheet is depicted in Figure 1.

1.2.1. Li^+ precipitation by $Al(OH)_3$

The Li+precipitation by $Al(OH)_3$ was conducted in a 500 mL two-necked flask equipped with a water bath, a magnetic stirrer, a thermometer, and a pH electrode. Firstly, 300 mL waste liquid of rock salt brine was added to the two-necked flask, and then a certain amount

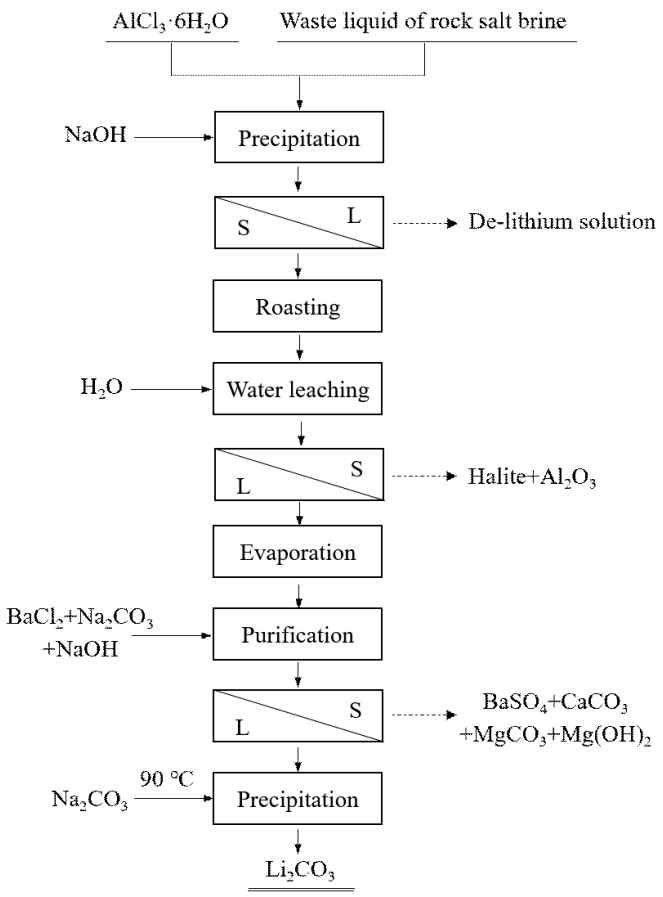

Fig. 1. Flowsheet for lithium recovery from waste liquid of rock salt brine

Rys. 1. Schemat odzysku litu z cieczy odpadowej solanki kamiennej

of $AlCl_3 \cdot 6H_2O$ salt was weighed according to the controlled Al^{3+}/Li^+ mole ratio and added into the prepared waste liquid. The resulting solutions were stirred at the controlled temperature (25, 40, 60, and 80°C) with a stirring rate of 100 rpm for a while to ensure the complete dissolution of $AlCl_3 \cdot 6H_2O$. Subsequently, 1 mol/L NaOH solution was dropped into the stirring solutions under the control of Na^+/Al^{3+} mole ratio with a drop rate of 3 mL/min using a peristaltic pump. After the NaOH drops stopped, the slurry was stirred for another 60 min to ensure the complete precipitation of Li^+. Finally, the precipitates were collected by suction filtration and then dried at 80°C for 24 h. The structure of the dried precipitates was determined by X-ray diffraction analysis (Ultima IV, Rigaku). The filtrates were collected and analysed by ICP-OES to detect Li^+ concentration.

1.2.2. Roasting and water leaching

The dried precipitates were roasted at a calcination temperature of 400°C for 40 min to ensure the complete transfer from insoluble to soluble lithium. Then, the roasting products were leached with deionised water (solid/liquid mass ratio of 1:2) for 30 min using a laboratory shaker with a shaking rate of 200 rpm. After water leaching, suction filtration was carried out and the obtained filtrates were enriched with Li^+, and its main chemical compositions were measured by ICP-OES.

1.2.3. Evaporation and Li_2CO_3 precipitation

The evaporation tests of the obtained filtrates were conducted to increase the concentration of Li^+ by continuous heating at 80°C in the drying oven, and the concentrated filtrates were separated from the precipitates by suction filtration. Subsequently, $BaCl_2$ and Na_2CO_3 were added into the evaporated solution to remove SO_4^{2-}, Ca^{2+}, and Mg^{2+} at room temperature (Swain 2016; Wang et al. 2017), and mole ratios of $BaCl_2/SO_4^{2-}$ and $Na_2CO_3/(Ca^{2+} + Mg^{2+})$ were both theoretical values of 1. Then, the pH of the evaporated solution was adjusted to 11.5 by adding NaOH to remove the residual Mg^{2+}. After SO_4^{2-}, Ca^{2+} and Mg^{2+} removal, the evaporated solution was precipitated at 90°C using Na_2CO_3 solid with $Na_2CO_3/2Li^+$ mole ratio of 1.05 for 30 min. Then, precipitates were filtered, washed, and dried at 80°C for 24 h, and then the Li_2CO_3 product was obtained and characterised by XRF (ARL Perform'X, Thermo Scientific).

The recovery of Li^+ in each process was calculated as follows

$$\text{Recovery (\%)} = \frac{V_i C_i}{V_0 C_0} \cdot 100\% \tag{4}$$

- V_0 – is the volume of the raw waste liquid of rock salt brine,
- V_i – is the volume of the obtained solution after each step,
- C_0 and C_i – are Li^+ concentrations of raw waste liquid and the obtained solution after each step, respectively.

2. Thermodynamic approach

To find the optimal conditions for the recovery of lithium in the stage of Li^+ precipitation by $Al(OH)_3$, the thermodynamic analyses of the simulated Li^+–Al^+–Mg^{2+}–Cl^-–H_2O system were conducted to construct the potential-pH (φ-pH) diagrams. The chemical compositions of the simulated Li^+–Al^+–Mg^{2+}–Cl^-–H_2O system were equaled to the actual waste liquid of rock salt brine after adding $AlCl_3 \cdot 6H_2O$ and NaOH solution, which consisted of [Al] = 0.033 mol/L, [Mg] = 0.00046 mol/L, [Li] = 0.013 mol/L, [Cl] = 6 mol/L in the opti-

mal conditions of Al^{3+}/Li^{+} = 2.5 and Na^{+}/Al^{3+} = 2.2 (displayed in chapters 3.2.1 and 3.2.2). In the simulated Li^{+}–Al^{+}–Mg^{2+}–Cl^{-}–H_2O system, the main species of Mg were Mg^{2+} and $Mg(OH)_2$ corresponding to the different pH values (Perrault 1974), and the main species of Al were Al^{3+}, $Al(OH)_3$ and AlO_2^{-}, but in the presence of Li^{+} and Cl^{-}, $Al(OH)_3$ and AlO_2^{-} became unstable and formed $LiCl \cdot 2Al(OH)_3 \cdot 2H_2O$ salt (Li et al. 2009; Kotsupalo et al. 2013). As described above, the equilibrium reactions in the system could be concluded as follows,

$$2H^{+} + 2e \rightarrow H_2 \tag{5}$$

$$O_2 + 4H^{+} + 4e \rightarrow 2H_2O \tag{6}$$

$$Al^{3+} + 3e \rightarrow Al \tag{7}$$

$$LiCl \cdot 2Al(OH)_3 \cdot 2H_2O + 6H^{+} \rightarrow 2Al^{3+} + Li^{+} + Cl^{-} + 8H_2O \tag{8}$$

$$2Al + Li^{+} + Cl^{-} + 8H_2O \rightarrow LiCl \cdot 2Al(OH)_3 \cdot 2H_2O + 6H^{+} + 6e \tag{9}$$

$$Mg^{2+} + 2e \rightarrow Mg \tag{10}$$

$$Mg^{2+} + 2H_2O \rightarrow Mg(OH)_2 + 2H^{+} \tag{11}$$

$$Mg + 2H_2O \rightarrow Mg(OH)_2 + 2H^{+} + 2e \tag{12}$$

According to the *Atlas of Electrochemical Equilibria in Aqueous Solutions* (Pourbaix 1974), the equilibrium reactions in the metal-water system were divided into three types as follows,

1. In the presence of H^{+} but no electron transfer, the formula is $aA + nH^{+} \rightarrow bB + cH_2O$ (equilibrium reactions 8 and 11). Due to no electron transfer, the electric potential φ was not involved in the calculation. Its formula is as follows,

$$pH = \frac{-\Delta_r G^{\theta}_m}{2.303nRT} - \frac{1}{n}\lg\frac{[B]^b}{[A]^a} \tag{13}$$

   - $\Delta_r G^{\theta}{}_m$ – is the standard Gibbs free energy of the reaction (kJ/mol),
   - R – is the molar gas constant (value is 8.314 J/(K · mol)),
   - T – is the temperature in Kelvins (K).

   In the φ-pH diagrams, the equilibrium reaction is a line perpendicular to the pH axis (*x*-axis).

2. In the presence of electron transfer, but no H^+ involved, the formula is $aA + ze \rightarrow bB$ (equilibrium reactions 7 and 10). Due to no H^+ involved, the electric potential φ was not related to pH, and its formula is as follows,

$$\varphi = \frac{-\Delta_r G_m^\theta}{zF} - \frac{0.0591}{z} \lg \frac{[B]^b}{[A]^a} \tag{14}$$

   - F is the Faraday constant (value is 96485.3383 ± 0.0083 C/mol). In the φ-pH diagrams, the equilibrium reaction is a line parallel to the pH axis (*x*-axis).

3. In the presence of H^+ and electron transfer, the formula is $aA + nH^+ + ze \rightarrow bB + cH_2O$ (equilibrium reactions 5, 6, 9 and 12). The electric potential φ is expressed as,

$$\varphi = \frac{-\Delta_r G_m^\theta}{zF} - \frac{0.0591}{z} \lg \frac{[B]^b}{[A]^a} - \frac{0.0591n}{z} \text{pH} \tag{15}$$

   In the φ-pH diagrams, the equilibrium reaction is a line related to potential φ and pH.

The standard Gibbs free energy of the reaction $\Delta_r G^\theta{}_m$ can be calculated using the following formula

$$\Delta_r G^\theta{}_m = \sum v_i \Delta_f G^\theta \tag{16}$$

- $\Delta_f G^\theta$ – is the standard Gibbs free energies of formation,
- v_i – is the stoichiometric coefficient (value positive for reaction product, value negative for reactant).

The standard Gibbs free energies of formation $\Delta_f G^\theta$ at 298.15 K of the involved ions and compounds containing Li, Al, Mg, and Cl were taken from *Lange's Handbook of Chemistry* (Speight 2005) as shown in Table 1.

Unfortunately, the standard Gibbs free energy of formation $\Delta_f G^\theta$ for $LiCl \cdot 2Al(OH)_3 \cdot 2H_2O$ salt was not reported in the literature or handbook, so its $\Delta_f G^\theta$ will be predicted. Mostafa et al. (1995) developed a group contributions method to predict the standard heat and Gibbs free energies of the formation of solid inorganic salts. The group contributions method was suitable for the inorganic salts with complex molecular structures. The prediction $\Delta_f G^\theta$ of $LiCl \cdot 2Al(OH)_3 \cdot 2H_2O$ salt was the summation of the given $\Delta_f G^\theta$ for the different decomposed groups (Li^+, Cl^-, $2Al^{3+}$, $6OH^-$ and $2H_2O$) and was equal to –3095.612 kJ/mol after calculation.

According to the formula (13)–(15) and the retrieved $\Delta_f G^\theta$, $\Delta_r G^\theta{}_m$ value and its pH or electric potential φ of the equilibrium reactions (5)–(12) can be calculated successively.

Table 1. The thermochemical data ($\Delta_f G^\theta$ at 298.15 K, G^θ and calculated $\Delta_f G^\theta$ at 298.15, 323.15, 348.15 and 373.15 K) of the ions and compounds containing Li, Al, Mg, Cl (kJ/mol)

Tabela 1. Dane termochemiczne ($\Delta_f G^\theta$ w temperaturze 298,15 K, G^θ i obliczone $\Delta_f G^\theta$ w temperaturze 298,15, 323,15, 348,15 i 373,15 K) jonów i związków zawierających Li, Al, Mg, Cl (kJ/mol)

Substances	$\Delta_f G^\theta_{298.15}$ in Reference	$G^\theta_{298.15}$	$G^\theta_{323.15}$	$G^\theta_{348.15}$	$G^\theta_{373.15}$	Calculated $\Delta_f G^\theta_{298.15}$	Calculated $\Delta_f G^\theta_{323.15}$	Calculated $\Delta_f G^\theta_{348.15}$	Calculated $\Delta_f G^\theta_{373.15}$	Error (%)
Al	0	–8.455	–9.192	–9.970	–10.799	0	0	0	0	0
Al^{3+}	–485.3	–416.910	–407.660	–399.167	–391.414	–485.596	–481.770	–477.978	–474.231	0.06
Li^+	–292.30	–275.705	–275.646	–275.939	–276.596	–292.733	–293.972	–295.290	–296.714	0.15
Cl^-	–131.3	–190.301	–192.017	–193.277	–194.081	–131.335	–128.193	–124.786	–121.107	0.03
H^+	0	6.241	6.642	6.797	6.709	0	0	0	0	0
O_2	0	–61.159	–66.316	–71.532	–76.802	0	0	0	0	0
H_2	0	–38.945	–42.243	–45.592	–48.995	0	0	0	0	0
H_2O	–237.14	–306.818	–308.631	–310.560	–312.603	–237.293	–233.229	–229.202	–225.207	0.06
Mg	0	–9.748	–10.590	–11.481	–12.419	0	0	0	0	0
Mg^{2+}	–454.8	–413.478	–409.242	–405.546	–402.377	–455.157	–454.181	–453.252	–452.369	0.08
$Mg(OH)_2$	–833.7	–943.918	–945.579	–947.392	–949.359	–833.594	–825.978	–818.362	–810.746	0.01
e	—	–25.713	–27.764	–29.594	–31.205	–	–	–	–	–

Then, the φ-pH diagram of the simulated Li^+–Al^+–Mg^{2+}–Cl^-–H_2O system on standard condition (298.15 K) can be constructed.

However, the φ-pH diagram of the simulated Li^+–Al^+–Mg^{2+}–Cl^-–H_2O system on the other temperature was difficult to construct due to the lack of standard Gibbs free energy of formation $\Delta_f G^\theta$ at the desired temperature in thermochemical data books. To solve this problem, the approximate prediction was conducted due to the linear relationship between $\Delta_f G^\theta$ and temperature, which can be expressed as

$$\Delta_f G^\theta = A + BT \tag{17}$$

- A – is the intercept of the fitting line,
- B – is the slope of the fitting line, and the fitting line can be fitted using the given $\Delta_f G^\theta$ at different temperatures.

Additionally, $\Delta_f G^\theta$ can be calculated according to its definition that $\Delta_f G^\theta$ is defined as Gibbs free energy variation during the transformation of stable simple substance to 1 mol compound under standard state, and can be expressed as

$$\Delta_f G^{\theta\,=} = \sum v_i G^\theta \tag{18}$$

- G^θ – is the standard Gibbs free energy,
- v_i – is the stoichiometric coefficient.

It should be noted that the standard Gibbs free energy of the electron (e) should be involved in the calculation formula (18).

The standard Gibbs free energies G^θ at 298.15 K, 323.15 K, 348.15 K and 373.15 K of the involved ions and compounds were taken from *Thermochemical properties of inorganic substances* (Barin et al. 1977) and the calculated $\Delta_f G^\theta$ was subsequently conducted as shown in Table 1. Then, the calculated $\Delta_f G^\theta_{298.15}$ according to calculation formula (18) was compared with the given $\Delta_f G^\theta_{298.15}$ from *Lange's Handbook of Chemistry*, which showed a minimal error of less than 0.15%, indicating extremely high accuracy and consistency.

Based on the calculation formula (17) and the calculated $\Delta_f G^\theta$ at 298.15, 323.15, 348.15, and 373.15 K in Table 1, the linear relationship between $\Delta_f G^\theta$ with temperature can be obtained (Table 2). The calculated $\Delta_f G^\theta$ at the desired temperature (298.15, 313.15, 333.15, and 353.15 K) was successfully carried out in Table 2. The standard Gibbs free energies of formation for simple substances (Al, H_2, O_2, and Mg) and H^+ are 0 according to its definition and thus are not displayed in Table 2. According to the group contributions method (Mostafa et al. 1995), $\Delta_f G^\theta$ of $LiCl \cdot 2Al(OH)_3 \cdot 2H_2O$ salt at 298.15, 313.15, 333.15, and 353.15 K were also predicted and shown in Table 2.

Finally, the φ-pH diagrams of the simulated Li^+–Al^+–Mg^{2+}–Cl^-–H_2O system at the desired temperature (298.15, 313.15, 333.15 and 353.15 K) were successfully constructed and displayed in Figure 2.

Table 2. The linear relationship between $\Delta_f G^\theta$ with temperature and the calculated $\Delta_f G^\theta$ at 298.15, 313.15, 333.15 and 353.15 K of the ions and compounds (kJ/mol)

Tabela 2. Liniowa zależność $\Delta_f G^\theta$ od temperatury i obliczonej $\Delta_f G^\theta$ przy 298,15, 313,15, 333,15 i 353,15 K jonów i związków (kJ/mol)

Substances	Linear relationship	R^2	$\Delta_f G^\theta_{298.15}$	$\Delta_f G^\theta_{313.15}$	$\Delta_f G^\theta_{333.15}$	$\Delta_f G^\theta_{353.15}$
Al^{3+}	$\Delta_f G^\theta = 0.15154T - 530.7602$	0.99997	–485.579	–483.305	–480.275	–477.244
Li^+	$\Delta_f G^\theta = -0.05304T - 276.8737$	0.99855	–292.688	–293.483	–294.544	–295.605
Cl^-	$\Delta_f G^\theta = 0.13637T - 172.1271$	0.99814	–131.468	–129.423	–126.695	–123.968
$LiCl \cdot 2Al(OH)_3 \cdot 2H_2O$	–	–	–3,095.612	–3,059.858	–3,012.186	–2,964.513
H_2O	$\Delta_f G^\theta = 0.16115T - 285.3222$	0.99998	–237.275	–234.858	–231.635	–228.412
Mg^{2+}	$\Delta_f G^\theta = 0.03717T - 466.2162$	0.99926	–455.134	–454.576	–453.833	–453.090
$Mg(OH)_2$	$\Delta_f G^\theta = 0.30463T - 924.41965$	1	–833.594	–829.025	–822.932	–816.840

Finally, the φ-pH diagrams of the simulated Li^+–Al^+–Mg^{2+}–Cl^-–H_2O system at the desired temperature (298.15, 313.15, 333.15 and 353.15 K) were successfully constructed and displayed in Figure 2.

According to Figure 2, the species of Al in the H_2O region were Al^{3+} and $LiCl \cdot 2Al(OH)_3 \cdot 2H_2O$ salt in the presence of Li^+ and Cl^- with the cut-off pH value varying from 6.45 to 6.51 as temperature increased from 298.15 K to 353.15 K. Moreover, the species of Mg in the H_2O region were Mg^{2+} and $Mg(OH)_2$, with cut-off pH values varying from 10.09 to 8.55 as temperature increased from 298.15 K to 353.15 K. The pH value of Li^+ precipitation by $Al(OH)_3$ should be located in the $LiCl \cdot 2Al(OH)_3 \cdot 2H_2O$ salt region with no formation of $Mg(OH)_2$, which was marked with a grey slant in Fig. 2. The initial pH of this region shown a slight variation as temperature changed and its value was ~6.5. The ended pH of this region showed a remarkable reduction from 10.09 to 8.55 as temperature increased, leading to the region's area continuously tightening.

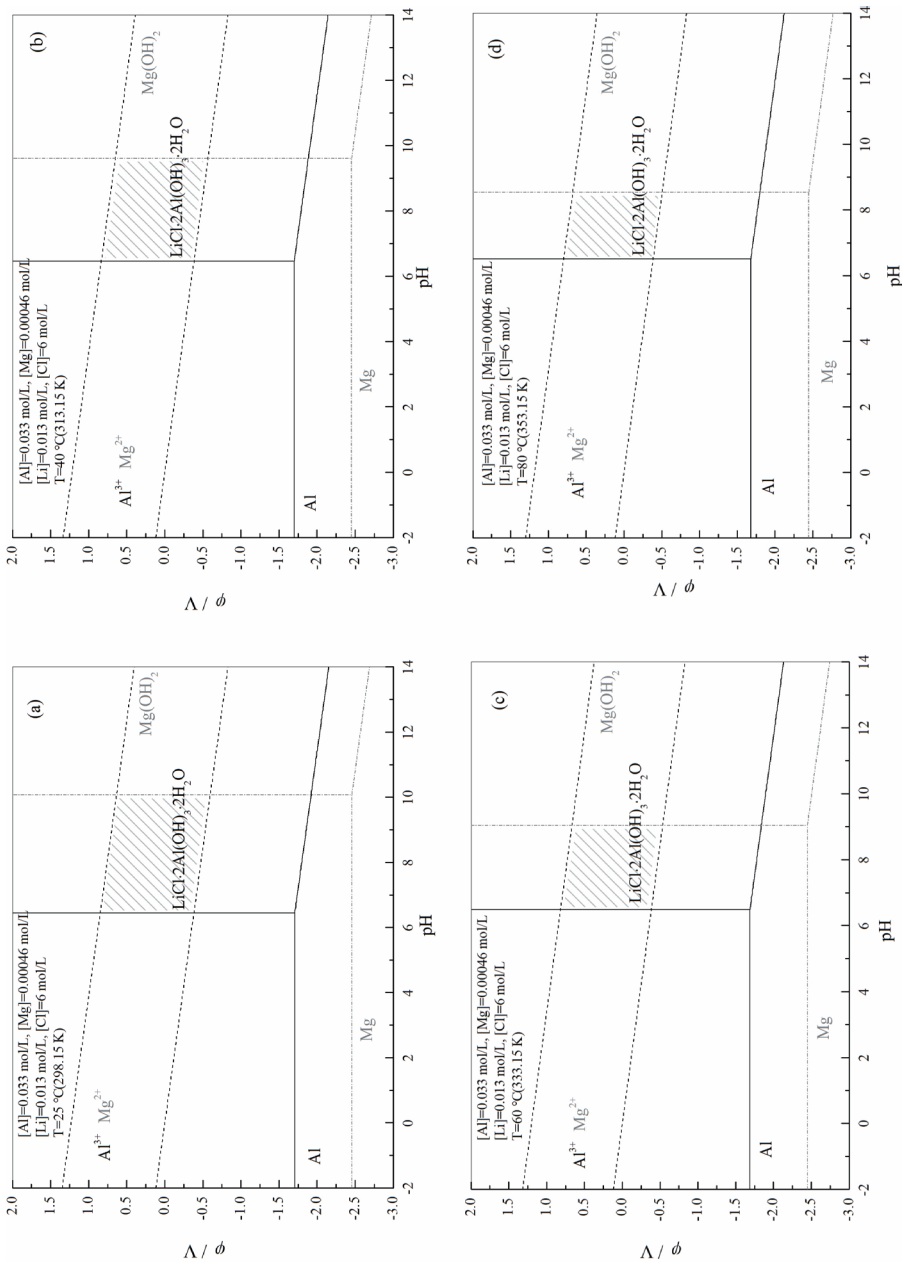

Fig. 2. φ-pH diagrams of the simulated Li^+–Al^+–Mg^{2+}–Cl^-–H_2O system at 298.15 K (a), 313.15 K(b), 333.15 K(c) and 353.15 K(d)

Rys. 2. Wykresy φ-pH symulowanego układu Li^+–Al^+–Mg^{2+}–Cl^-–H_2O w temperaturach 298,15 K (a), 313,15 K(b), 333,15 K(c) i 353,15 K(d)

3. Results

3.1. Chemical compositions

Table 3 shows the chemical compositions of the studied waste liquid of rock salt brine. The concentration of Li^+ was 0.099 g/L, and the main impurities were composed of a small amount of Ca^{2+}, Mg^{2+}, B^{3+}, and a large amount of Na^+, K^+, Cl^-, SO_4^{2-}. The Mg^{2+}/Li^+ mss ratio was meager (0.12), and the concentrations of Na^+ and Cl^- were close to the saturated NaCl solution.

Table 3. Chemical compositions (g/L) of waste liquid of rock salt brine

Tabela 3. Skład chemiczny (g/L) cieczy odpadowej solanki kamiennej

Constituent	Na^+	K^+	Ca^{2+}	Mg^{2+}	Li^+	B^{3+}	Cl^-	SO_4^{2-}	Mg^{2+}/Li^+ mss ratio	Density (g/mL)	pH
Content	120.3	6.1	0.049	0.012	0.099	0.41	170.9	34.4	0.12	1.2177	9.8

3.2. Li^+ precipitation by $Al(OH)_3$

3.2.1. Al^{3+}/Li^+ mole ratio

The actual reaction of the Li precipitation by $Al(OH)_3$ in the system can be divided into two stages:

1. In the first stage, with the addition of $AlCl_3 \cdot 6H_2O$ under a controlled Al^{3+}/Li^+ mole ratio into the waste liquid of rock salt brine, $AlCl_3 \cdot 6H_2O$ dissolved and produced Al^{3+} and Cl^-. pH of the resulting solution decreased remarkably from 9.8 to strong acid (pH = 0.5~2).
2. Secondly, NaOH solution was dropped slowly into the resulting solutions under a controlled Na^+/Al^{3+} mole ratio, and the pH of the mixed solution slowly increased from strong acid to near neutral. The dissolved Al^{3+} is transferred to amorphous $Al(OH)_3$, which can catch Li^+ and Cl^- in layers to form $LiCl \cdot 2Al(OH)_3 \cdot xH_2O$ salt at pH = ~6.5 (shown in Figure 2).

According to the chemical reaction formula (1) of Li^+ precipitation by $Al(OH)_3$, the theoretical mole ratio of Al^{3+}/Li^+ and Na^+/Al^{3+} was 2 and 3, respectively. The stoichiometric coefficient of water in chemical reaction formula (1) and $LiCl \cdot 2Al(OH)_3 \cdot xH_2O$ salt was unascertained, and its value in *Chapter 1 Thermodynamic approach* was 2 for convenient calculation.

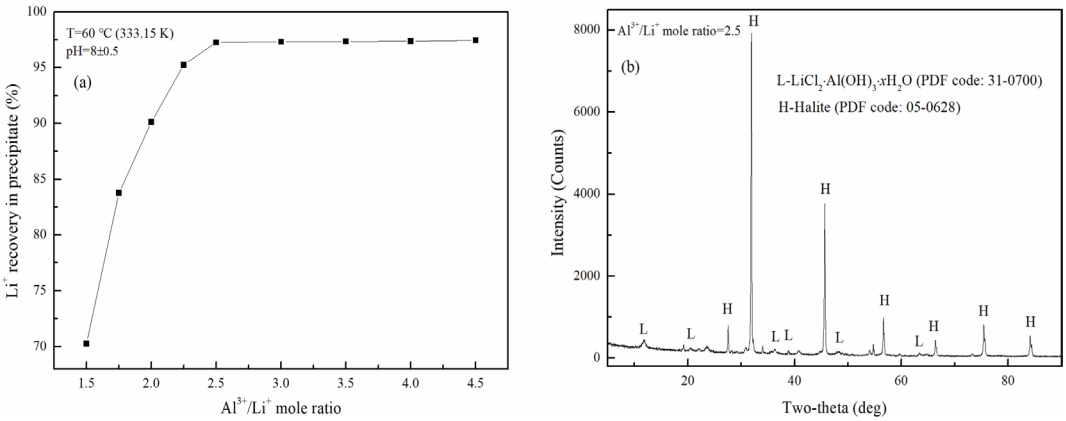

Fig. 3. The influence of Al^{3+}/Li^{+} mole ratio on Li^{+} recovery in precipitate (a) and XRD pattern (b) of the dried precipitates at Al^{3+}/Li^{+} mole ratio = 2.5, pH = 8±0.5 and T = 60°C

Rys. 3. Wpływ stosunku molowego Al^{3+}/Li^{+} na odzysk Li+ w osadzie (a) i widmie XRD (b) wysuszonych osadów przy stosunku molowym Al^{3+}/Li^{+} = 2,5, pH = 8±0,5 i T = 60°C

The influence of the Al^{3+}/Li^{+} mole ratio affecting Li^{+} recovery in the precipitate was shown in Figure 3(a), which showed a growing trend as the Al^{3+}/Li^{+} mole ratio increased from 1.5 to 2.5 and then remained at a constant value of about 97% when Al^{3+}/Li^{+} mole ratio is more than 2.5. The optimal Al^{3+}/Li^{+} mole ratio can be selected as 2.5, corresponding to the Li^{+} recovery in the precipitate of 97.25%, indicating nearly whole Li^{+} in the waste liquid of rock salt brine was precipitated by $Al(OH)_3$ on this condition.

XRD pattern of the dried precipitates at an optimal Al^{3+}/Li^{+} mole ratio of 2.5 was also displayed in Figure 3(b), which mainly consisted of a superior amount of halite with strong and sharp characteristic peaks and a small amount of $LiCl \cdot 2Al(OH)_3 \cdot xH_2O$ salt with weak and mild characteristic peaks. The superior amount of halite was generated by the additional Na^{+} and Cl^{-} when adding NaOH solution and $AlCl_3 \cdot 6H_2O$ into the raw waste liquid of rock salt brine with approximate saturated NaCl solution.

3.2.2. Na^{+}/Al^{3+} mole ratio

Figure 4 displayed the influence of Na^{+}/Al^{3+} mole ratio on Li^{+} recovery in the precipitate. The Na^{+}/Al^{3+} mole ratio was controlled by adding NaOH solution, so the pH value varied simultaneously. As the Na^{+}/Al^{3+} mole ratio increased from 1.4 to 3.0, the pH value increased linearly from 5.56 to 9.68, yet Li^{+} recovery in precipitate increased sharply firstly and then decreased slightly.

At pH = 5.56 (Na^{+}/Al^{3+} mole ratio = 1.4), Li^{+} recovery in the precipitate was only 46.86%, indicating that about half of Li^{+} in the waste liquid of rock salt brine was not recycled on this condition. The unacceptable Li^{+} recovery was due to the insufficient amorphous

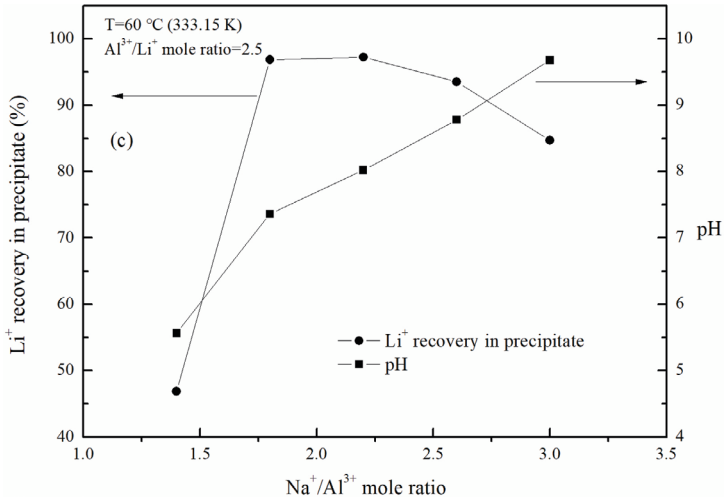

Fig. 4. The influence of Na^+/Al^{3+} mole ratio on Li^+ recovery in precipitate and pH at Al^{3+}/Li^+ mole ratio = 2.5 and T = 60°C

Rys. 4. Wpływ stosunku molowego $Na^+/Al3+$ na odzysk Li+ w osadzie i pH przy stosunku molowym Al^{3+}/Li^+ = 2,5 i T = 60°C

$Al(OH)_3$ products when pH is less than ~6.5 (initial pH value of $LiCl \cdot 2Al(OH)_3 \cdot 2H_2O$ formation in φ-pH diagram in Figure 2). Then as Na^+/Al^{3+} mole ratio increased from 1.4 to 1.8 (pH = 7.36), Li^+ recovery in precipitate increased nearly twice and reached up to 96.86%, which was close to 100%. Afterward, Li^+ recovery in precipitate increased slightly to a maximum value of 97.25% at Na^+/Al^{3+} mole ratio = 2.2 (pH = 8.02) and then decreased gradually to 84.71% at Na^+/Al^{3+} mole ratio = 3.0 (pH = 9.68). The decreased Li^+ recovery in precipitate at Na^+/Al^{3+} mole ratio = 3.0 was due to the transformation of the reaction product by NaOH and $AlCl_3 \cdot 6H_2O$ from amorphous $Al(OH)_3$ to bayerite, gibbsite or $Al(OH)_3$ crystal, which could not catch Li^+ and Cl^- in structure. In addition, suction filtration of these precipitates at Na^+/Al^{3+} mole ratio = 3.0 was more difficult than at Na^+/Al^{3+} mole ratio = 1.4~2.2, and its suction filtration time (~30 min) was about six times that at Na^+/Al^{3+} mole ratio = 1.4~2.2 (~5 min), which was caused by the formation of flocculent $Mg(OH)_2$ precipitate at higher pH value (pH = 9.68), which was confirmed by φ-pH diagram that $Mg(OH)_2$ was initially formed at pH = 9.05 on this condition (T = 60°C(333.15 K)). Therefore, the optimal Na^+/Al^{3+} mole ratio was 1.8~2.2, corresponding to pH = 7.36~8.02, which was located in the $LiCl \cdot 2Al(OH)_3 \cdot 2H_2O$ salt region with no formation of $Mg(OH)_2$ marked with grey slant in Figure 2.

3.2.3. Precipitation temperature and time

The influence of precipitation time at different temperatures on Li+ recovery in the precipitate was shown in Figure 5. According to the φ-pH diagram (Figure 2) in the simulated

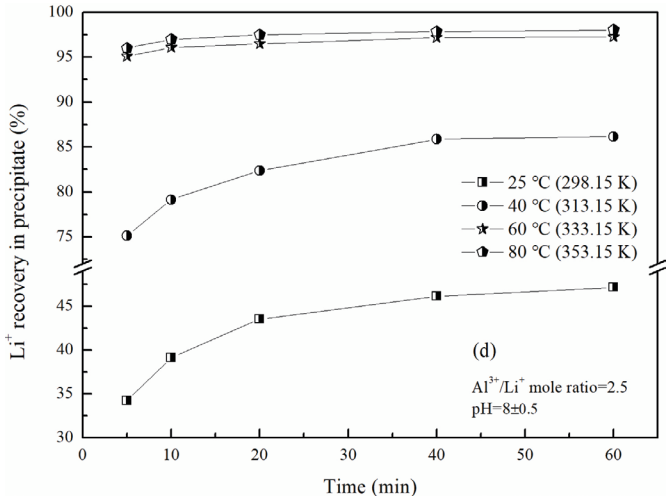

Fig. 5. The influence of precipitation time at different temperatures on Li^+ recovery in precipitate at Al^{3+}/Li^+ mole ratio = 2.5 and pH = 8±0.5

Rys. 5. Wpływ czasu wytrącania w różnych temperaturach na odzysk Li+ z osadu przy stosunku molowym Al3+/Li+ = 2,5 i pH = 8±0,5

Li^+–Al^+–Mg^{2+}–Cl^-–H_2O system, the initial pH of LiCl · 2Al(OH)3 · xH_2O salt formation was about 6.5. Then, Li^+ was gradually precipitated by the continuously generated amorphous $Al(OH)_3$ until the controlled Na^+/Al^{3+} mole ratio was reached. Then, the precipitation time was carried out to ensure the complete Li^+ precipitation. As precipitation time prolonged, Li^+ recovery in precipitate increased at different extents, which was also affected by temperature. At room temperature (25°C) and 40°C, Li^+ recovery in the precipitate was significantly impacted by time, showing a remarkable increasing trend at the first 20 min and a gentle increasing trend later. At 25°C, Li^+ recovery in the precipitate was much lower, varying from 34.21% (5 min) to 47.15% (60 min), and the increase rate of Li^+ recovery in the precipitate was getting slower and slower until it stopped, indicating unacceptable precipitation efficiency. At 40°C, Li^+ recovery in precipitate varied from 75.12% (5 min) to 86.14% (60 min). Moreover, it reached above 95% at 60 and 80°C at only 5 min, indicating significant precipitation efficiency improvement by temperature. The fast reaction rate at higher temperatures (60 and 80°C) required less precipitation to reach the ideal Li^+ recovery. According to Figure 5, the recommended precipitation temperature and time was 60°C for more than 20 min, and its Li^+ recovery in the precipitate was above 97%.

3.3. Roasting and water leaching

The obtained precipitates with Li^+ recovery of 97.25% on the optimal condition were roasted at the required temperature for enough time, accompanied by the complete transfer

from $LiCl \cdot 2Al(OH)_3 \cdot xH_2O$ salt to soluble LiCl and Al_2O_3. Subsequently, the roasting products were leached with water to obtain the solution with enriched Li^+ compared to the raw waste liquid, whose main chemical compositions are shown in Table 4.

Table 4. Main chemical compositions of raw waste liquid, enriched Li^+ solution and evaporated solution before and after SO_4^{2-}, Ca^{2+} and Mg^{2+} removal (g/L)

Tabela 4. Główne składy chemiczne surowej cieczy odpadowej, wzbogaconego roztworu Li^+ i odparowanego roztworu przed i po usunięciu SO_4^{2-}, Ca^{2+} i Mg^{2+} (g/L)

Element	Li^+	Mg^{2+}	SO_4^{2-}	Ca^{2+}	B^{3+}	Li^+ recovery (%)
Raw waste liquid	0.099	0.012	34.40	0.049	0.410	–
Enriched Li^+ solution	1.951	0.073	48.10	0.221	0.127	85.52
Evaporated solution before SO_4^{2-}, Ca^{2+} and Mg^{2+} removal	15.44	0.512	53.20	1.641	0.854	83.56
Evaporated solution after SO_4^{2-}, Ca^{2+} and Mg^{2+} removal	14.05	0.005	0.131	0.012	0.108	76.03

As shown in Table 4, the Li^+ concentration of enriched Li^+ solution (1.951 g/L) was 19.7 times that of raw waste liquid (0.099 g/L), indicating a remarkable concentration of Li^+. In consideration of the volume variation, the recovery of Li^+ in the Li^+ precipitation, roasting, and water leaching process was 85.52% in total, accompanied by Li^+ mass loss of 14.48%, which consisted of 2.75% loss in the Li^+ precipitation stage and 11.73% loss in roasting, and water leaching stage.

The concentrations of unwanted elements Mg^{2+}, SO_4^{2-}, Ca^{2+} and B^{3+} in enriched Li^+ solution were 6.08, 1.40, 4.51, and 0.31 times than that in raw waste liquid, whose values were less than that of Li^+ (19.7 times), indicating the effective removal of unwanted elements, especially for element B^{3+} and SO_4^{2-}.

3.4. Evaporation and Li_2CO_3 precipitation

The concentrate of Li^+ in the enriched Li^+ solution (1.951 g/L) did not meet the requirement of Li_2CO_3 production by precipitation method using sodium carbonate (Li^+ should exceed 10 g/L), which needs further evaporation. Subsequently, continuous heating was conducted to evaporate the enriched Li solution, and then $BaCl_2$, Na_2CO_3 and NaOH were successively added into the evaporated solution to remove SO_4^{2-}, Ca^{2+} and Mg^{2+}. The chemical compositions of the evaporated solution before and after SO_4^{2-}, Ca^{2+} and Mg^{2+} removal were also shown in Table 4.

As shown in Table 4, the concentration of Li^+ in evaporated solution before SO_4^{2-}, Ca^{2+} and Mg^{2+} removal was enriched to 15.44 g/L, about 7.9 times that in the enriched Li^+ solution. The unwanted elements (SO_4^{2-}, Ca^{2+} and Mg^{2+}) were concentrated simultaneously but effectively removed by adding $BaCl_2$, Na_2CO_3, and NaOH, whose concentrations were very low. The recovery of Li^+ in the evaporated process was 83.56%, indicating a slight amount of Li (~1.96%) was co-precipitated with halite (identified by XRD pattern) during evaporation (Liu et al. 2014). After SO_4^{2-}, Ca^{2+}, and Mg^{2+} removal, the recovery of Li^+ decreased to 76.03%, showing a 7.53% mass loss of Li^+ in this process, which was attributed to the entrainment of Li^+ adhering to the produced $BaSO_4$, $CaCO_3$, $MgCO_3$, and $Mg(OH)_2$ precipitates.

Subsequently, the evaporated solution after SO_4^{2-}, Ca^{2+}, and Mg^{2+} removal was used to precipitate Li_2CO_3 using Na_2CO_3 solid with $Na_2CO_3/2Li^+$ mole ratio of 1.05. The concentration of Li^+ in the solution after Li_2CO_3 precipitation was still 1.73 g/L, suggesting that only 87.69% Li^+ was precipitated by Na_2CO_3, and the total recovery of Li^+ was 66.69% after the whole experimental process. The chemical composition of the precipitated Li_2CO_3 product is displayed in Table 5. The precipitated Li_2CO_3 product has 99.3% Li_2CO_3 with limited impurities, which meets the requirement of the Li_2CO_3–0 product in standard GB/T 11075-2013.

Table 5. Chemical composition of the precipitated Li_2CO_3 product

Tabela 5. Skład chemiczny wytrąconego produktu Li_2CO_3

Constituent	Li_2CO_3	Na	Fe	Ca	Mg	SO_4^{2-}	Cl^-
Li_2CO_3 product content (%)	99.3	0.032	0.0015	0.021	0.012	0.110	0.010
Li_2CO_3 product content without purification (%)	86.8	0.048	0.0019	5.35	1.560	4.291	0.018
Li_2CO_3–0 product content in GB/T 11075–2013 (%)	≥99.2	≤0.08	≤0.0020	≤0.025	≤0.015	≤0.200	≤0.010

For comparison, the evaporated solution without purification was used to precipitate Li_2CO_3 in the same conditions, and the chemical composition of the precipitated Li_2CO_3 is also displayed in Table 5. The lower Li_2CO_3 content and the large amount of Ca, Mg and SO_4^{2-} showed the unacceptable application in the energy vehicle industry.

3.5. Mass balance and economic viability

The mass balance of the lithium recovery from the waste liquid of rock salt brine was created according to the experiment results and displayed in Table 6. It seems that 1 ton Li_2CO_3 will consume a lot of raw waste liquid and chemicals, and the cost is estimated as 35,000~45,000 RMB/t in China, which was a little higher than the adsorption method (30,000~35,000 RMB/t), but lower than the electrodialysis method (60,000 RMB/t), showing competitive economic benefits. Additionally, the treatment and comprehensive utilization of byproducts can be further considered. The byproducts of Li^+ precipitation consisted of 3,676 mg/L Br, 1,310 mg/L B_2O_3, and 0.96% KCl, which was higher than the industrial grade in standard DZ/T 0212.2–2020 (Br ≥ 300 mg/L, B_2O_3 ≥ 1,000 mg/L and KCl ≥ 0.5~1.0%), thus such valuable elements (Br, B and K) can be recycled in the future. The byproducts of Li_2CO_3 precipitation still contained 1.73 g/L Li^+, which can be added into the evaporation process to improve the total recovery of Li^+. The large amount of Al_2O_3 in the byproducts of water leaching can be dissolved by NaOH solution to form $NaAlO_2$, which can replace some $AlCl_3 \cdot 6H_2O$ in the Li^+ precipitation process. Considering the recycling of byproducts, the total recovery of Li^+ will be expected to be greater than 75%.

Table 6. Mass balance of 1 ton Li_2CO_3 production (ton)

Tabela 6. Bilans masowy 1 tony produkcji Li_2CO_3 (tona)

Chemicals	Li^+ precipitation	Roasting	Water leaching	Evaporation	Purification	Li_2CO_3 precipitation
Waste liquid	2,530	–	–	–	–	–
$AlCl_3 \cdot 6H_2O$	21.78	–	–	–	–	–
NaOH	7.93	–	–	–	0.02	–
H_2O	198.48	–	21.82	–	0.5	–
Heat (°C)	60	400	RT	80	RT	90
$BaCl_2$	–	–	–	–	8.99	–
Na_2CO_3	–	–	–	–	0.44	1.53
Products	16.85	10.91	20.87	2.20	1.65	1
Byproducts	2,741.34	5.94	11.86	18.67	10.50	2.18

3.6. Comparison of methods for lithium recovery

From Table 7, the total recovery of Li^+ in this study was higher than that of the co-precipitation method and was roughly close to that of solvent extraction, membrane, and carbonate precipitation methods, but lower than that of adsorption and electrodialysis methods. The Li_2CO_3 purities by membrane, co-precipitation, carbonate precipitation, and this study were higher than 99.2% (Li_2CO_3–0 product). The promising lithium recovery and Li_2CO_3 purity of waste liquid of rock salt brine show the extreme potential of a new type of lithium resource.

Table 7. Lists the comparison of Li_2CO_3 purity and lithium recovery using different methods

Tabela 7. Zestawienie porównania czystości Li_2CO_3 i odzysku litu różnymi metodami

Methods	Li^+ in brine (g/L)	Li_2CO_3 purity (%)	Li^+ recovery (%)	References
Adsorption*	0.36	–	~91	Paranthaman et al. 2017
Solvent extraction*	10	–	70.4	Song et al. 2020
Electrodialysis*	1.99	–	85.3	Xiong et al. 2021
Membrane	2.05	99.6	68.7	Xu et al. 2017
Co-precipitation	6.09	99.7	57.99	Wang et al. 2017
Carbonate precipitation	0.76~0.84	99.55	~72	An et al. 2012
This study	0.099	99.3	>75	This study

* The Li^+ recovery of the adsorption, solvent extraction and electrodialysis methods only represented the lithium extraction from brine and was not conducted to concentration, purification and Li_2CO_3 precipitation process, so Li_2CO_3 purity was not displayed in references.

Conclusions

An integrated process consisting of Li^+ precipitation by $Al(OH)_3$, roasting and water leaching, evaporation, and Li_2CO_3 precipitation was successfully carried out to recycle Li^+ from the waste liquid of rock salt brine. In the Li^+ precipitation by $Al(OH)_3$ stage, the recovery of Li^+ reached 97.25% on the optimal condition of Al^{3+}/Li^+ mole ratio = 2.5, Na^+/Al^{3+} mole ratio = 2.2, precipitation temperature of 60°C (333.15 K) for more than

20 min. According to the φ-pH diagrams of the simulated Li^+–Al^+–Mg^{2+}–Cl^-–H_2O system, the pH value should be located in the $LiCl \cdot 2Al(OH)_3 \cdot 2H_2O$ salt region with no formation of $Mg(OH)_2$, which started at pH = ~6.5, and ended at pH from 10.09 to 8.55 as temperature increased from 298.15 K to 353.15 K. In the roasting and water leaching stage, the concentration of Li^+ was enriched to 1.951 g/L, 19.7 times that of raw waste liquid (0.099 g/L), accompanied by the recovery of Li^+ of 85.52%. Then, the solution was further evaporated, and the concentration of Li^+ reached 15.44 g/L. Finally, the evaporated solution after SO_4^{2-}, Ca^{2+} and Mg^{2+} removal was conducted for Li_2CO_3 precipitation, and the obtained Li_2CO_3 product has 99.3% Li_2CO_3 with the limited impurities, which meets the requirement of the Li_2CO_3–0 product in standard GB/T 11075-2013. The above success in lithium recovery using the aluminum hydroxide precipitation method provided a promising lithium extraction method from the waste liquid of rock salt brine, which could be regarded as a new type of lithium resource, showing an environment-friendly and resource-saving prospect.

Project Supported by Technology Project of Chongqing Planning and Natural Resources Bureau (Grant No. KJ-2023008) and Scientific and Technological Research Program of Chongqing Municipal Education Commission (Grant No. KJQN202101434 and Grant No. KJQN202301423). Thanks to school funding of Yangtze Normal University.

The Authors have no conflicts of interest to declare.

REFERENCES

An et al. 2012 – An, J.W., Kang, D.J., Tran, K.T., Kim, M.J., Lim, T. and Tran, T. 2012. Recovery of lithium from Uyuni salar brine. *Hydrometallurgy* 117–118, pp.64–70, DOI: 10.1016/j.hydromet.2012.02.008.

Barin et al. 1977 – Barin, I., Knacke, O. and Kubaschewski, O. 1977. *Thermochemical properties of inorganic substances*. Berlin: Springer Berlin Heidelberg.

Chung et al. 2008 – Chung, K., Lee, J., Kim, W., Kim, S. and Cho, K. 2008. Inorganic adsorbent containing polymeric membrane reservoir for the recovery of lithium from seawater. *Journal of Membrane Science* 325(2), pp. 503–508, DOI: 10.1016/j.memsci.2008.09.041.

Han et al 2018 – Han, B., Porvali, A., Lundström, M. and Louhi-Kultanen, M. 2018. Lithium Recovery by Precipitation from Impure Solutions – Lithium Ion Battery Waste. *Chemical Engineering & Technology* 41(6), pp. 1205–1210, DOI: 10.1002/ceat.201700667.

He et al. 2017 – He, L., Xu, W., Song, Y., Liu, X. and Zhao, Z. 2017. Selective removal of magnesium from a lithium-concentrated anolyte by magnesium ammonium phosphate precipitation. *Separation and Purification Technology* 187, pp. 214–220, DOI: 10.1016/j.seppur.2017.04.028.

IEA 2024. *Global Critical Minerals Outlook 2024*. Paris:International Energy Agency.

Kotsupalo et al. 2013 – Kotsupalo, N.P., Ryabtsev, A.D., Poroshina, I.A., Kurakov, A.A., Mamylova, E.V., Menzheres, L.T. and Korchagin, M.A. 2013. Effect of Structure on the Sorption Properties of Chlorine-containing Form of Double Aluminum Lithium Hydroxide. *Russian Journal of Applied Chemistry* 86(4), pp. 482−487, DOI: 10.1134/S1070427213040046.

Li et al. 2009 – Li, Q., Jensen, J.O. and Bjerrum, N.J. 2009. Chemistry, electrochemistry, and electrochemical applications: aluminum. *Encyclopedia of Electrochemical Power Sources*, pp. 695–708, DOI: 10.1016/B978-044452745-5.00951-5.

Li et al. 2019 – Li, H., Eksteen, J. and Kuang, G. 2019. Recovery of lithium from mineral resources: State-of-the-art and perspectives – A review. *Hydrometallurgy* 189, pp. 105–129, DOI: 10.1016/j.hydromet.2019.105129.

Li et al. 2020 – Li, X., Chen, L., Chao, Y., Chen, W., Luo, J., Xiong, J., Zhu, F., Chu, X., Li, H. and Zhu, W. 2020. Amorphous TiO_2-Derived Large-Capacity Lithium Ion Sieve for Lithium Recovery. *Chemical Engineering & Technology* 43(9), pp. 1784–1791, DOI: 10.1002/ceat.201900374.

Liu et al. 2014 – Liu, Y., Guo, Y., Yu, X., Wang, S. and Deng, T. 2014. Solid-Liquid Metastable Phase Equilibria in the Five-Component System (Li plus Na plus K+Cl+SO_4+H_2O) at 308.15 K. *Journal of Chemical & Engineering Data* 59(5), pp. 1685–1691, DOI: 10.1021/JE500140E.

Liu et al. 2022 – Liu, Y., Ma, B., Lv, Y., Wang, C. and Chen, Y. 2022. Selective recovery and efficient separation of lithium, rubidium, and cesium from lepidolite ores. *Separation and Purification Technology* 288, DOI: 10.1016/j.seppur.2022.120667.

Ma, P. and Zhang, P. 1999. Lithium resources in china's salt lakes & its sustainable development. *Bulletin of the Chinese Academy of Sciences* 13(4), pp. 225–229

Meng et al. 2019 – Meng, F., McNeice, J., Zadeh, S.S. and Ghahreman, A. 2019. Review of Lithium Production and Recovery from Minerals, Brines, and Lithium-Ion Batteries. *Mineral Processing and Extractive Metallurgy Review* 42, pp. 123–141, DOI: 10.1080/08827508.2019.1668387.

Mostafa et al. 1995 – Mostafa, A.T.M.G., Eakman, J.M. and Yarbro, S.L. 1995. Prediction of Standard Heats and Gibbs Free Energies of Formation of Solid Inorganic Salts from Group Contributions. *Industrial & Engineering Chemistry Research* 34(12), pp. 4577–4582, DOI: 10.1021/IE00039A053.

NBSC 2023. *China Statistical Yearbook* 2023. Beijing: National Bureau of Statistics of China (NBSC).

Paranthaman et al. 2017 – Paranthaman, M.P., Li, L., Luo, J., Hoke, T., Ucar, H., Moyer, B.A. and Harrison, S. 2017. Recovery of Lithium from Geothermal Brine with Lithium – Aluminum Layered Double Hydroxide Chloride Sorbents. *Environmental Science & Technology* 51, pp. 13481–13486, DOI: 10.1021/acs.est.7b03464.

Perrault, G.G. 1974. The potential-pH diagram of the magnesium-water system. *Electroanalytical Chemistry and Interfacial Electrochemistry*, 51, pp. 107–119, DOI: 10.1016/S0022-0728(74)80298-6.

Pourbaix, M. 1974. *Atlas of Electrochemical Equilibria in Aqueous Solutions(2nd English edn)*. Houston: National Association of Corrosion Engineers.

Song et al. 2020 – Song, Y., Zhao, Z. and He, L. 2020. Lithium recovery from Li_3PO_4 leaching liquor: Solvent extraction mechanism of saponified D2EHPA system. *Separation and Purification Technology* 249, pp. 117161.

Speight, J.G. 2005. *Lange's Handbook of Chemistry (16th ed.)*. McGRAW-HILL.

Swain, B. 2016. Recovery and recycling of lithium: A review. *Separation and Purification Technology* 172, pp. 388–403, DOI: 10.1016/j.seppur.2016.08.031.

Wang et al. 2017 – Wang, H., Zhong, Y., Du, B., Zhao, Y. and Wang, M. 2017. Recovery of both magnesium and lithium from high Mg/Li ratio brines using a novel process. *Hydrometallurgy* 175, pp. 102–108, DOI: 10.1016/j.hydromet.2017.10.017.

Xiong et al. 2021 – Xiong, J., He, L., Liu, D., Xu, W. and Zhao, Z. 2021. Olivine-$FePO_4$ preparation for lithium extraction from brines via Electrochemical De-intercalation/Intercalation method. *Desalination* 520, DOI: 10.1016/j.desal.2021.115326.

Xu et al. 2020 – Xu, W., Liu, D., He, L. and Zhao, Z. 2020. A Comprehensive Membrane Process for Preparing Lithium Carbonate from High Mg/Li Brine. *Membranes* 10(12), DOI: 10.3390/membranes10120371.

Yu et al. 2014 – Yu, J., Zheng, M., Wu, Q., Nie, Z. and Bu, L. 2014. Lithium Extraction from Carbonate-type Saline Lake by Utilizing of Geothermal Solar Pond in Tibet. *Acta Geologica Sinica (English Edition)* 88(S1), pp. 389–390.

Zhong et al. 2021 – Zhong, J., Lin, S. and Yu, J. 2021. Li^+ adsorption performance and mechanism using lithium/aluminum layered double hydroxides in low grade brines. *Desalination* 505, DOI: 10.1016/j.desal.2021.114983.

RECOVERY OF LITHIUM FROM WASTE LIQUID OF ROCK SALT BRINE USING ALUMINUM HYDROXIDE PRECIPITATION METHOD

Keywords

lithium recovery, waste liquid of rock salt brine,
aluminum hydroxide precipitation method, thermodynamic analysis

Abstract

An integrated process consisting of Li^+ precipitation by $Al(OH)_3$, roasting, water leaching, evaporation, and Li_2CO_3 precipitation was used to recycle Li^+ from the waste liquid of rock salt brine (0.099 g/L Li^+). Waste liquid from rock salt brine was discharged wastewater after NaCl crystallization and the removal of impurities in the salt manufacturing plant of the good rock salt mine. The influences of Al^{3+}/Li^+ mole ratio, Na^+/Al^{3+} mole ratio, precipitation temperature, and time on the recovery of Li^+ were investigated during Li^+ precipitation by $Al(OH)_3$ stage. The results showed that the optimal condition was Al^{3+}/Li^+ mole ratio = 2.5, Na^+/Al^{3+} mole ratio = 2.2, precipitation temperature of 60°C (333.15 K) for more than 20 min, whose recovery of Li^+ reached 97.25%. The thermodynamic analyses of the simulated Li^+–Al^+–Mg^{2+}–Cl^-–H_2O system were conducted to construct the potential-pH (φ-pH) diagrams. The results showed that the pH value should be located in the $LiCl \cdot 2Al(OH)_3 \cdot 2H_2O$ salt region with no formation of $Mg(OH)_2$, which started at pH = ~6.5 and ended at pH from 10.09 to 8.55 as the temperature changed. Subsequently, the Li+precipitate was roasting for the transformation of insoluble $LiCl \cdot 2Al(OH)_3 \cdot xH_2O$ salt to soluble LiCl, followed by the water leaching to obtain the enriched Li^+ solution (1.951 g/L Li^+) with Li^+ recovery of 85.52%. To meet the requirement of Li_2CO_3 precipitation, the enriched Li^+ solution was evaporated, and Na_2CO_3 was added to precipitate the Li_2CO_3 product after SO_4^{2-}, Ca^{2+}, and Mg^{2+} removal. The total recovery of Li^+ was 66.69% after the experimental process, and the purity of Li_2CO_3 product was 99.3%, which can be regarded as industrial-grade Li_2CO_3. In conclusion, the success in lithium recovery using the aluminum hydroxide precipitation method provided a new perspective for preparing Li_2CO_3 from the waste liquid of rock salt brine, which could be considered as a newly developing lithium resource to meet the dramatically increasing demand for lithium in new energy vehicle industry.

ODZYSK LITU Z CIECZY ODPADOWEJ SOLANKI KAMIENNEJ METODĄ WYTRĄCANIA WODOROTLENKIEM GLINU

Słowa kluczowe

odzysk litu, ciecz odpadowa solanki z soli kamiennej,
metoda wytrącania wodorotlenkiem glinu, analiza termodynamiczna

Streszczenie

Do recyklingu Li^+ z cieczy odpadowej solanki kamiennej zastosowano zintegrowany proces obejmujący wytrącanie Li^+ przez $Al(OH)_3$, prażenie, ługowanie wodą, odparowywanie i wytrącanie Li_2CO_3 (0,099 g/l Li^+). Płyn odpadowy z solanki soli kamiennej odprowadzano do ścieków po krystalizacji NaCl i usunięciu zanieczyszczeń w zakładzie produkcji soli kopalni soli kamiennej Dobra. Badano wpływ stosunku molowego Al^{3+}/Li^+, stosunku molowego Na^+/Al^{3+}, temperatury i czasu wytrącania na odzysk Li^+ podczas wytrącania Li^+ w etapie $Al(OH)_3$. Wyniki wykazały, że optymalnymi warunkami był stosunek molowy Al^{3+}/Li^+ = 2,5, stosunek molowy Na^+/Al^{3+} = 2,2, temperatura wytrącania 60°C (333,15 K) przez ponad 20 min, przy czym odzysk Li^+ osiągnął 97,25%. Przeprowadzono analizy termodynamiczne symulowanego układu Li^+–Al^+–Mg^{2+}–Cl^-–H_2O w celu skonstruowania wykresów potencjał-pH (φ-pH). $LiCl \cdot 2Al(OH)_3 \cdot 2H_2O$ obszar soli bez tworzenia $Mg(OH)_2$, który rozpoczął się przy pH = ~6,5 i zakończył przy pH od 10,09 do 8,55 wraz ze zmianą temperatury. Następnie osad Li^+ prażono w celu przekształcenia nierozpuszczalnej soli $LiCl \cdot 2Al(OH)_3 \cdot xH_2O$ w rozpuszczalny LiCl, a następnie ługowano wodą w celu uzyskania wzbogaconego roztworu Li^+ (1,951 g/L Li^+) z uzyskiem Li^+ wynoszącym 85,52 %. Aby spełnić wymagania dotyczące wytrącania Li_2CO_3, wzbogacony roztwór Li^+ odparowano i dodano Na_2CO_3 w celu wytrącenia produktu Li_2CO_3 po usunięciu SO_4^{2-}, Ca^{2+} i Mg^{2+}. Całkowity odzysk Li^+ po procesie eksperymentalnym wyniósł 66,69%, a czystość produktu Li_2CO_3 wyniosła 99,3%, co można uznać za Li_2CO_3 klasy przemysłowej. Podsumowując, sukces w odzyskiwaniu litu metodą wytrącania wodorotlenkiem glinu otworzył nową perspektywę przygotowania Li_2CO_3 z cieczy odpadowej solanki z soli kamiennej, który można uznać za nowo rozwijające się źródło litu w celu zaspokojenia dramatycznie rosnącego zapotrzebowania na lit w przemyśle pojazdów wykorzystujących nowe źródła energii.